WATERMARKING GRAPH NEURAL NETWORKS VIA EXPLANATIONS FOR OWNERSHIP PROTECTION

Anonymous authors
Paper under double-blind review

ABSTRACT

Graph Neural Networks (GNNs) are widely deployed in industry, making their intellectual property valuable. However, protecting GNNs from unauthorized use remains a challenge. Watermarking offers a solution by embedding ownership information into models. Existing watermarking methods have two limitations: First, they rarely focus on graph data or GNNs. Second, the *de facto* backdoor-based method relies on manipulating training data, which can introduce ownership ambiguity through misclassification and vulnerability to data poisoning attacks that can interrupt the backdoor mechanism. Our explanation-based watermarking inherits the strengths of backdoor-based methods (e.g., black-box verification) without data manipulation, eliminating ownership ambiguity and data dependencies. In particular, we watermark GNN explanations such that these explanations are statistically distinct from others, so ownership claims must be verified through statistical significance. We theoretically prove that, even with full knowledge of our method, locating the watermark is NP-hard. Empirically, our method demonstrates robustness to fine-tuning and pruning attacks. By addressing these challenges, our approach significantly advances GNN intellectual property protection.

1 INTRODUCTION

Graph Neural Networks (GNNs) (Scarselli et al., 2008; Kipf & Welling, 2017; Hamilton et al., 2018; Veličković et al., 2018) are widely used for graph-structured data tasks, such as social network analysis, bioinformatics, and recommendation systems (Zhang et al., 2021; Zhou et al., 2020). Various giant companies have depend on GNNs: Amazon for product recommendations (Virinchi, 2022); Google's TensorflowGNN for Maps traffic prediction (Sibon Li et al., 2021; Oliver Lange, 2020); Meta for friend/content recommendations (MetaAI, 2023); Alibaba's AliGraph for fraud and risk detection (Yang, 2019; Liu et al., 2021b; Li, 2019). Given significant GNN development, ownership verification is crucial to protect against illegal copying, model theft, and malicious distribution.

Watermarking embeds secret patterns into models (Uchida et al., 2017) to verify ownership. As a *de facto* approach, backdoor-based watermarking (Adi et al., 2018; Bansal et al., 2022; Lv et al., 2023; Yan et al., 2023; Li et al., 2022; Shao et al., 2022; Lansari et al., 2023) insert the watermark pattern as a "trigger" into clean samples with altered *target labels*, and trains on both watermarked and clean data. During verification, ownership is demonstrated by producing the triggered samples that yield the target label. Backdoor-based watermarking methods have several merits: they are robust to removal attacks (pruning and fine-tuning), and verification only requires black-box model access.

However, recent works (Yan et al., 2023; Liu et al., 2024; Xu et al., 2023) reveal a fundamental limitation: backdoor-based methods induce ownership ambiguity, as attackers could falsely claim misclassified data as ownership evidence. Additionally, embedding watermarks into data properties creates vulnerability to data poisoning attacks, where an adversary can manipulate the data to disrupt the watermarking process Steinhardt et al. (2017); Zhang et al. (2019). Recognizing these limitations, researchers have explored alternate watermark embedding spaces. (Shao et al., 2024) embed watermarks DNN prediction *explanations*, avoiding tampering with predictions or parameters. While offering a compelling alternative to backdoor-based watermarking, their approach assumes a known ground-truth watermark, introducing challenges like a third-party verification requirement and potential disputes over the true watermark. Moreover, they do not address graph data's unique complexities, including structural dependencies and multi-hop relationships.

We extend explanation-based watermarks to GNNs, additionally addressing graph-specific challenges and avoiding the need of a ground-truth watermark for verification. Our approach aligns explanations of selected subgraphs with a predefined watermark, ensuring robustness to removal attacks and preserving advantages of explanation-based methods. In doing so, we present the first explanation-based watermarking method tailored to GNNs.

Our approach: We develop a novel watermarking strategy for protecting GNN model ownership that both inherits the merits from and mitigates the drawbacks of backdoor-based watermarking. Like backdoor-based methods, our approach only needs black-box model access. However, in contrast to using *predictions* on the *polluted* watermarked samples, we leverage the *explanations* of GNN predictions on *clean* samples and align them with a predefined watermark for ownership verification.

Before training, the owner selects secret watermarked subgraphs (private) and defines a watermark pattern (*possibly* private).[1] The GNN trains with a dual-objective loss function that minimizes (1) classification loss, and (2) distance between the watermark and watermarked subgraph explanations. Like GraphLIME (Huang et al., 2023), we use Gaussian kernel matrices to approximate node feature influence on predictions. However, instead of an iterative approach, we use ridge regression to compute feature attribution vectors in a single step, providing a more efficient, closed-form solution.

Our approach is (i) *Effective*: Explanations of watermarked subgraphs exhibit high similarity to the watermark after training. (ii) *Unique:* This similarity across explanations is statistically unlikely without watermarking, and hence serves as our ownership evidence. (iii) *Undetectable:* We prove that, even with full knowledge of our watermarking method, finding the private watermarked subgraphs is computationally intractable (NP-hard). (iv) *Robust:* Empirical evaluations on multiple benchmark graph datasets and GNN models demonstrate robustness to fine-tuning and pruning-based watermark removal attacks. We summarize our contributions as follows:

- We introduce the first known method for watermarking GNNs via their explanations, eliminating ownership ambiguity and avoiding data manipulation problems of black-box watermarking schemes.
- We prove that it is NP-hard for the worst-case adversary to identify our watermarking mechanism.
- We show our method is robust to watermark removal attacks like fine-tuning and pruning.

2 Related Work

White-Box Watermarking. These techniques (Darvish Rouhani et al., 2019; Uchida et al., 2017; Wang & Kerschbaum, 2020; Shafieinejad et al., 2021) directly embed watermarks into the model parameters or features during training. For example, Uchida et al. (2017) embed a watermark via a regularization term, while Darvish Rouhani et al. (2019) propose embedding the watermark into the activation/feature maps. Although these methods are robust in theory (Chen et al., 2022), they require full access to the model parameters during verification, which may not be feasible in real-world scenarios, especially for deployed models operating in black-box environments (e.g., APIs).

Black-Box Watermarking. Black-box approaches verify model ownership using only model predictions (Adi et al., 2018; Chen et al., 2018; Szyller et al., 2021; Le Merrer et al., 2019). They often use backdoor mechanisms, training models to output specific predictions for "trigger" inputs as ownership evidence (Adi et al., 2018; Zhang et al., 2018). These methods have significant downsides. First, watermarks embedded into data features can be interrupted by data poisoning attacks (Steinhardt et al., 2017; Zhang et al., 2019). Further, backdoor methods suffer from ambiguity — attackers may claim naturally-misclassified samples as their own "watermark"(Yan et al., 2023; Liu et al., 2024). Given these issues with backdoor-based methods, Shao et al. (2024) proposed embedding DNN watermarks in explanations to avoid prediction manipulation and maintain black-box compatibility.

Watermarking GNNs. Varying size and structure of graphs make watermark embedding challenging. Moreover, GNNs' multi-hop message-passing mechanisms are more sensitive to data changes than neural networks processing more uniform data like images or text (Wang & Gong, 2019; Zügner et al., 2020; Zhou et al., 2023). The only existing black-box watermarking GNNs (Xu et al., 2023) suffers from the same issue as backdoor watermarking of non-graph models (Liu et al., 2024) [2]. These issues,

[1] Ownership verification does not require knowledge of the watermark pattern.

[2] Recent "fingerprinting" method (Waheed et al., 2024) verifies GNN ownership with node embeddings instead of explicit watermark patterns. However, it is vulnerable to pruning attacks. Relying on intrinsic model features can limit uniqueness guarantees and risk ownership ambiguity (Wang et al., 2021; Liu et al., 2024).

coupled with the complexity of graphs, make existing watermarking techniques unsuitable for GNNs. This highlights the need for novel watermarking schemes.

3 Background and Problem Formulation

3.1 GNNs for Node Classification

Let a graph be denoted as $G = (\mathcal{V}, \mathcal{E}, \mathbf{X})$, where $\mathcal{V}$ is the set of nodes, $\mathcal{E}$ is the set of edges, and $\mathbf{X} = [\mathbf{x}_1, \cdots, \mathbf{x}_N] \in \mathbb{R}^{N \times F}$ is the node feature matrix. $N = |\mathcal{V}|$ is the number of nodes, F is the number of features per node, and $\mathbf{x}_u \in \mathbb{R}^F$ is the node u's feature vector. We assume the task of interest is node classification. In this context, each node $v \in \mathcal{V}$ has a label y_v from a label set $\mathcal{C} = \{1, 2, \cdots, C\}$, and we have a set of $|\mathcal{V}^{tr}|$ labeled nodes $(\mathcal{V}^{tr}, \mathbf{y}^{tr}) = \{(v_u^{tr}, y_u^{tr})\}_{u \in \mathcal{V}^{tr}} \subset \mathcal{V} \times \mathcal{C}$ nodes as the training set. A GNN for node classification takes as input the graph G and training nodes $\mathcal{V}^{tr}$, and learns a node classifier, denoted as f, that predicts the label $\hat{y}_v$ for each node v. Suppose a GNN has L layers and a node v's representation in the l-th layer is $\mathbf{h}_v^{(l)}$, where $\mathbf{h}_v^{(0)} = \mathbf{x}_v$. Then it updates $\mathbf{h}_v^{(l)}$ for each node v using the following two operations:

$$\mathbf{l}_v^{(l)} = \texttt{Agg}\big(\{\mathbf{h}_u^{(l-1)} : u \in \mathcal{N}(v)\}\big),\ \mathbf{h}_v^{(l)} = \texttt{Comb}\big(\mathbf{h}_v^{(l-1)}, \mathbf{l}_v^{(l)}\big), \tag{1}$$

where `Agg` aggregates representations of a node's neighbors, and `Comb` combines a node's previous representation and aggregated representation of that aggregation to update the node representation. $\mathcal{N}(v)$ denotes the neighbors of v. Different GNNs use different `Agg` and `Comb` operations.

The last-layer representation $\mathbf{h}_v^{(L)} \in \mathbb{R}^{|C|}$ of training nodes $v \in \mathcal{V}^{tr}$ are used to train the node classifier f. Let Θ be the model parameters and v's softmax scores be $\mathbf{p}_v = f_\Theta(\mathcal{V}^{tr})_v = \text{softmax}(\mathbf{h}_v^{(L)})$, where $p_{v,c}$ is the probability of v being class c. Θ are learned by minimizing a classification (e.g., cross-entropy) loss on the training nodes:

$$\Theta^* = \arg\min_\Theta \mathcal{L}_{CE}(\mathbf{y}^{tr}, f_\Theta(\mathcal{V}^{tr})) = -\Sigma_{v \in \mathcal{V}^{tr}} \ln p_{v,y_v}. \tag{2}$$

3.2 GNN Explanation

GNN explanations identify graph features that influence predictions. Some methods (e.g., GNNExplainer (Ying et al., 2019) and PGExplainer (Luo et al., 2020)) identify important subgraphs, while others (e.g., GraphLime (Huang et al., 2023)) identify key node features. Inspired by GraphLime (Huang et al., 2023), we use Gaussian kernel matrices to capture relationships between node features and predictions: Gaussian kernel matrices effectively capture nonlinear dependencies and complex variable relationships, ensuring subtle patterns in the data are effectively represented Yamada et al. (2012). Using these Gaussian kernel matrices, we employ a closed-form solution with ridge regression (Hoerl & Kennard, 1970) to compute feature importance in a single step.

Our function $explain(\cdot)$ takes node feature matrix $\mathbf{X}$ and softmax scores $\mathbf{P} = [\mathbf{p}_1, \cdots, \mathbf{p}_N]$, yielding F-dimensional attribution vector $\mathbf{e}$ showing each feature's influence on predictions across nodes. This computes feature attributions ($\mathbf{e}$) by leveraging the relationships between input features ($\mathbf{X}$) and output predictions ($\mathbf{P}$) through Gaussian kernel matrices.

$$\mathbf{e} = explain(\mathbf{X}, \mathbf{P}) = (\tilde{\boldsymbol{K}}^T \tilde{\boldsymbol{K}} + \lambda \boldsymbol{I}_F)^{-1} \tilde{\boldsymbol{K}}^T \tilde{\boldsymbol{L}}. \tag{3}$$

We defer precise mathematical definitions to Appendix B. For high-level understanding, the matrix $\tilde{\boldsymbol{K}}$ ($N^2 \times F$) encodes pairwise feature similarities between nodes via a Gaussian kernel. $\tilde{\boldsymbol{L}}$ ($N^2 \times 1$) uses a Gaussian kernel to encode pairwise prediction similarities between nodes. The term $(\tilde{\boldsymbol{K}}^T \tilde{\boldsymbol{K}} + \lambda \boldsymbol{I}_F)^{-1}$, where λ is a regularization hyperparameter and $\boldsymbol{I}_F$ is the $F \times F$ identity matrix, solves a ridge regression problem to ensure a stable and interpretable solution. The product $\tilde{\boldsymbol{K}}^T \tilde{\boldsymbol{L}}$ ($F \times 1$) ties the Gaussian feature similarities ($\tilde{\boldsymbol{K}}$) to the output prediction similarities ($\tilde{\boldsymbol{L}}$), ultimately yielding the vector $\mathbf{e}$ ($F \times 1$), which quantifies the importance of each input feature for the GNN's predictions. This kernel-based method allows us to (1) aggregate node-level predictions into subgraph-level information; (2) utilize GNN-predicted probabilities over all categories; and (3) compared to GNNExplainer (Ying et al., 2019), keep the watermark subgraph private.

In this paper, the *explanation* of a GNN's node predictions means this feature attribution vector $\mathbf{e}$.

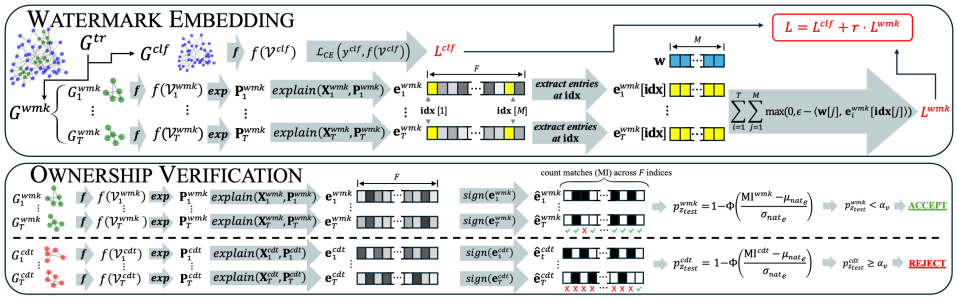

Figure 1: Overview: During embedding, f is optimized to (1) minimize node classification loss and (2) align watermarked subgraph explanations with $\mathbf{w}$. The similarity of G^{cdt}'s binarized explanations, $\{\hat{\mathbf{e}}_i^{cdt}\}_{i=1}^{T}$, is tested for significance during ownership verification. In this example, G^{cdt} are *not* the watermarked subgraphs; therefore, $\{\hat{\mathbf{e}}_i^{cdt}\}_{i=1}^{T}$ fail to exhibit significant similarity and are rejected.

3.3 Problem Formulation

We propose an explanation-based GNN watermarking method. Our approach defines a watermark pattern ($\mathbf{w}$) and selects subgraphs from G. The GNN f is trained to embed the relationship between $\mathbf{w}$ and these subgraphs, enabling their explanations to act as verifiable ownership evidence.

Threat Model: There are three parties: the model owner, the adversary, and the third-party model ownership verifier. Obviously, the model owner has white-box access to the target GNN model.

- **Adversary:** We investigate an adversary who falsely claims to own GNN model f. We assume they lacks knowledge of the watermarked subgraphs in G, but we also evaluate robustness under challenging scenarios where they might know specific details (e.g., shape or number of watermarked subgraphs). The adversary tries to undermine the watermark by (1) searching for the watermarked subgraphs (or similarly-convincing alternatives), or (2) implementing a removal attack.
- **Model Ownership Verifier:** Following existing backdoor-based watermarking, we use black-box ownership verification, where the verifier does not need full access to the protected model.

Objectives: Our explanation-based watermarking method aims to achieve the below objectives:

1. **Effectiveness.** Training must embed the watermark in the explanations of our selected subgraphs: their feature attribution vectors must be *sufficiently*[3] aligned with vector $\mathbf{w}$.
2. **Uniqueness.** Aligning watermarked subgraph explanations with $\mathbf{w}$ must yield statistically-significant similarity between explanations that is unlikely to occur in alternate solutions.
3. **Robustness.** The watermark must be robust to removal attacks like fine-tuning and pruning.
4. **Undetectability.** Non-owners should be unable to locate the watermarked explanations.

4 Methodology

Our watermarking method has three stages: (1) design, (2) embedding, and (3) ownership verification. We introduce stages (2) and (3) first as design relies on them.

Training f uses a dual-objective loss function balancing node classification and watermark embedding. Minimizing watermark loss aligns $\mathbf{w}$ with explanations of f's predictions on watermarked subgraphs, embedding the watermark. Verification tests for explanations statistically-significant similarity from their common alignment with $\mathbf{w}$. Lastly, we detail a watermark design that ensures this statistical significance, which provides unambiguous ownership evidence. Figure 1 overviews our method.

4.1 Watermark Embedding

Let training set $\mathcal{V}^{tr}$ be split as two disjoint subsets: $\mathcal{V}^{clf}$ for node classification and $\mathcal{V}^{wmk}$ for watermarking. Select T subgraphs $\{G_1^{wmk}, \ldots, G_T^{wmk}\}$ whose nodes $\{\mathcal{V}_i^{wmk}\}_{i=1}^{T}$ will be watermarked.

[3]Note: alignment between explanations and $\mathbf{w}$ is a tool for the owner to measure optimization success; for a watermark to function as ownership evidence, alignment must simply be "good enough" (See Section 5.2.1).

These subgraphs have explanations $\{\mathbf{e}_1^{wmk}, \ldots, \mathbf{e}_T^{wmk}\}$, where $\mathbf{e}_i^{wmk} = explain(\mathbf{X}_i^{wmk}, \mathbf{P}_i^{wmk})$ explains f's softmax output $\mathbf{P}_i^{wmk}$ on G_i^{wmk}'s nodes $\mathcal{V}_i^{wmk}$, with features $\mathbf{X}_i^{wmk}$. Define watermark $\mathbf{w}$ as an M-dimensional vector ($M \leq F$), with entries of 1s and -1s.

Inspired by Shao et al. (2024), we use multi-objective optimization to balance classification performance with a hinge-like *watermark loss*. Minimizing this loss encourages alignment between $\mathbf{w}$ and $\{\mathbf{e}_i^{wmk}\}_{i=1}^T$, embedding the relationship between $\mathbf{w}$ and these subgraphs.

$$\mathcal{L}_{wmk}(\{\mathbf{e}_i^{wmk}\}_{i=1}^T, \mathbf{w}) = \Sigma_{i=1}^T \Sigma_{j=1}^M \max(0, \epsilon - \mathbf{w}[j] \cdot \mathbf{e}_i^{wmk}[\mathbf{idx}[j]]), \tag{4}$$

where $\mathbf{e}_i^{wmk}[\mathbf{idx}]$ represents the *watermarked portion* of $\mathbf{e}_i^{wmk}$ on node feature indices $\mathbf{idx}$ with length M; $\mathbf{idx}$ is same for all explanations $\{\mathbf{e}_i^{wmk}\}_{i=1}^T$. We emphasize that $\mathbf{idx}$ are not arbitrary, but are rather the result of design choices discussed later in Section 4.3. The hyperparameter ϵ bounds the contribution of each multiplied pair $\mathbf{w}[j] \cdot \mathbf{e}_i^{wmk}[\mathbf{idx}[j]]$ to the summation.

We train the GNN model f to minimize both classification loss on the nodes $\mathcal{V}^{clf}$ (see Equation 2) and watermark loss on the explanations of $\{G_1^{wmk}, \ldots, G_T^{wmk}\}$, with a balancing hyperparameter r:

$$\min_{\Theta} \mathcal{L}_{CE}(\mathbf{y}^{clf}, f_\Theta(\mathcal{V}^{clf})) + r \cdot \mathcal{L}_{wmk}(\{\mathbf{e}_i^{wmk}\}_{i=1}^T, \mathbf{w}). \tag{5}$$

After training, the learned parameters Θ ensures not only an accurate node classifier, but also similarity between $\mathbf{w}$ and explanations $\{\mathbf{e}_i^{wmk}\}_{i=1}^T$ at indices $\mathbf{idx}$. See Algorithm 1 in Appendix for the details.

4.2 Ownership Verification

Since they were aligned with the same $\mathbf{w}$, explanations $\{\mathbf{e}_i^{cdt}\}_{i=1}^T$ will be similar to each other after training. Therefore, when presented with T *candidate subgraphs* $\{\mathbf{e}_1^{cdt}, \mathbf{e}_2^{cdt}, \cdots, \mathbf{e}_T^{cdt}\}$ by a purported owner (note that our threat model assumes a strong adversary who also knows T), we must measure the similarity between these explanations to verify ownership. If the similarity is statistically significant at a certain level, we can conclude the purported owner knows which subgraphs were watermarked during training, and therefore that they are the true owner.

Explanation Matching: Our GNN explainer in Equation (3) gives a positive or negative score for each node feature, indicating its influence on the GNN's predictions, generalized across all nodes in the graph. To easily compare these values across candidate explanations, we first *binarize* them with the sign function. For the j^{th} index of explanation $\mathbf{e}_i^{cdt}$, this process is defined as:

$$\hat{\mathbf{e}}_i^{cdt}[j] = \begin{cases} 1 & \text{if } \mathbf{e}_i^{cdt}[j] > 0, \\ -1 & \text{if } \mathbf{e}_i^{cdt}[j] < 0, \\ 0 & \text{otherwise.} \end{cases} \tag{6}$$

We then count the *matching indices* (MI) across all the binarized explanations — the number of indices at which all binarized explanations have matching, non-zero values:[4]

$$\text{MI}^{cdt} = \text{MI}(\{\hat{\mathbf{e}}_i^{cdt}\}_{i=1}^T) = \Sigma_{j=1}^F \mathbb{1}((\{\hat{\mathbf{e}}_i^{cdt}[j] \neq 0, \forall i\}) \wedge (\hat{\mathbf{e}}_1^{cdt}[j] = \cdots = \hat{\mathbf{e}}_T^{cdt}[j])). \tag{7}$$

Approximating a Baseline MI Distribution: To test MI^{cdt} significance, we first approximate the distribution of *naturally-occurring* matches: the MIs for all T-sized sets of un-watermarked explanations. This involves running I simulations (sufficiently large; $I = 1000$ in our experiments), where we randomly sample sets of T subgraphs from G and compute the MI of the binarized explanations for each set. We then derive *empirical* estimates of the mean and standard deviation, μ_{nat_e} and σ_{nat_e} (indicated by the subscript "e"), for the I MIs.

Significance Testing to Verify Ownership: We verify the purported owner's ownership by testing if MI^{cdt} is statistically unlikely for randomly selected subgraphs, at a significance level α_v:

$$Ownership = \begin{cases} True & \text{if } p_{z_{test}} < \alpha_v, \\ False & \text{otherwise.} \end{cases} \tag{8}$$

where $z_{test} = \frac{\text{MI}^{cdt} - \mu_{nat_e}}{\sigma_{nat_e}}$. Algorithm 2 (Appendix) details the ownership verification process.

[4]We exclude 0s from our MI count. A 0 in the explanation indicates no dependence between features and predictions, which could only result from extreme (unlikely) optimization precision. These 0s likely reflect existing 0s in $\mathbf{X}$, so we conclude they are irrelevant as watermarking metrics.

4.3 WATERMARK DESIGN

The watermark $\mathbf{w}$ is an M-dimensional vector with entries of 1 and -1. The size and location of $\mathbf{w}$ must allow us to *effectively* embed *unique* ownership evidence into GNN.

Design Goal: The watermark should be designed to yield a *target MI* (MI^{tgt}) that passes the statistical test in Equation (8). This value is essentially the upper bound on a one-sided confidence interval. However, since we cannot get the estimates μ_{nat_e} or σ_{nat_e} without a trained model, we instead use a binomial distribution to *predict* estimates μ_{nat_p} and σ_{nat_p} (note the subscript "p").

We assume the random case, where a binarized explanation includes values -1 or 1 with equal probability (again, ignoring zeros; see Footnote 4). Across T binarized explanations, the probability of a match at an index is $p_{match} = 2 \times 0.5^T$. We estimate $\mu_{nat_p} = F \times p_{match}$ (where F is number of node features), and $\sigma_{nat_p} = \sqrt{F \times p_{match}(1 - p_{match})}$. We therefore define MI^{tgt} as follows:

$$\text{MI}^{tgt} = min(\mu_{nat_p} + \sigma_{nat_p} \times z_{tgt}, F), \tag{9}$$

where z_{tgt} is the z-score for target significance α_{tgt}. In practice, we set $\alpha_{tgt} = 1e-5$; since MI^{tgt} affects watermark design, we want to ensure it does not underestimate the upper bound.

Watermark Length M: For T binarized explanations, our estimated lower bound of baseline MI is:

$$\text{MI}^{LB} = max(\mu_{nat_p} - \sigma_{nat_p} \times z_{LB}, 0), \tag{10}$$

where z_{LB} is the z-score for target significance, α_{LB} — in practice, α_{LB} equals α_{tgt} ($1e-5$).

We expect that our watermark must add ($\text{MI}^{tgt} - \text{MI}^{LB}$) net MI at most. However, natural matching between some indices in the binarized explanations may reduce the watermark's net contribution. We therefore pad watermark length.Padding is based on the probability of a natural match. In the worst case, where MI^{tgt} indices naturally match, the probability of a watermarked index producing a new match is $(F - \text{MI}^{tgt})/F$. Consequently, we pad the required M by the inverse, $F/(F - \text{MI}^{tgt})$:

$$M = \lceil (\text{MI}^{tgt} - \text{MI}^{LB}) \times F/(F - \text{MI}^{tgt}) \rceil. \tag{11}$$

Watermark length M should yield enough net MI to reach the total, MI^{tgt}, that the owner needs to demonstrate ownership. Note that under the assumption that we set α_{LB} equal to α_{tgt}, Equation (11) is ultimately a function of three variables: α_{tgt}, F, and T.

Watermark Location idx: Each explanation corresponds to node feature indices. It is easiest to watermark indices at non-zero features. We advise selecting **idx** from the M most frequently non-zero node features across all T watermarked subgraphs. Let $\mathbf{X}^{wmk} = [\mathbf{X}_1^{wmk}; \mathbf{X}_2^{wmk}; \cdots \mathbf{X}_T^{wmk}]$ be the concatenation of node features of the T watermarked subgraphs. Define **idx** as:

$$\mathbf{idx} = \text{top}_M \left(\left\{ \|\mathbf{x}_1^{wmk}\|_0, \|\mathbf{x}_2^{wmk}\|_0, \cdots, \|\mathbf{x}_F^{wmk}\|_0 \right\} \right), \tag{12}$$

where $\mathbf{x}_j^{wmk}$ is the j-th column of $\mathbf{X}^{wmk}$, $\|\cdot\|_0$ represents the number of non-zero entries in a vector, and $\text{top}_M(\cdot)$ returns the indices of the M largest values.

4.4 LOCATING THE WATERMARKED SUBGRAPHS

An adversary may attempt to locate watermarked subgraphs to claim ownership. In the worst case, they have access to G^{tr} and know T (number of watermarked subgraphs) and s (nodes per subgraph). With G^{tr}, they can compute the natural match distribution ($\mu_{nat_e}, \sigma_{nat_e}$) and search for T subgraphs with maximally significant MI, using either brute-force or random search.

Brute-Force Search: If the training graph has N nodes, identifying $n_{sub} = sN$-node subgraphs yields $\binom{N}{n_{sub}}$ options. To find the T subgraphs with a maximum MI across their binarized explanations, an adversary must compare all T-sized sets of these subgraphs, with $\binom{\binom{N}{n_{sub}}}{T}$ sets in total.

Moreover, we can reduce the Maximum k-Subset Intersection (MSI) Clifford & Popa (2011) problem to the that of a brute search for T effective subgraphs. MSI, known to be NP-hard, seeks the k subsets with maximal intersection. Our reduction maps each MSI subset to a potential subgraph in G, with k

Table 1: Watermarking results. Each value is the average of five trials with distinct random seeds.

	GCN		SGC		SAGE		Transformer	
	Acc (Train/test)		Acc (Train/test)		Acc (Train/test)		Acc (Train/test)	
Dataset	Wmk	No Wmk	Wmk	No Wmk	Wmk	No Wmk	Wmk	No Wmk
Photo	91.3 / 89.4	90.9 / 88.3	91.4 / 89.9	90.1 / 88.0	94.2 / 90.8	94.1 / 88.2	99.9 / 90.7	95.0 / 86.8
PubMed	88.6 / 85.8	85.7 / 81.4	88.8 / 85.9	85.3 / 81.4	90.5 / 86.0	91.1 / 81.2	99.7 / 87.9	94.2 / 86.5
CS	98.5 / 90.3	96.8 / 89.8	98.4 / 90.3	96.7 / 90.1	100.0 / 88.4	99.9 / 88.9	100.0 / 93.1	99.4 / 92.2
Reddit2	—	—	—	—	—	—	83.4 / 79.4	81.0 / 80.4
	Wmk Alignmt	MI p-val	Wmk Alignmt	MI p-val	Wmk Alignmt	MI p-val	Wmk Alignmt	MI (p-val)
Photo	91.4	<0.001	91.8	<0.001	97.7	<0.001	87.9	<0.001
PubMed	91.5	<0.001	88.9	<0.001	85.2	<0.001	94.0	<0.001
CS	73.8	<0.001	74.5	<0.001	78.2	<0.001	73.9	<0.001
Reddit2	—	—	—	—	—	—	76.3	<0.001

corresponding to our selected number of subgraphs, T. Finding k sets with maximum intersection corresponds to finding T subgraphs whose explanations share the maximum matching indices.

Random Search: Adversaries can search for a "good enough" group of subgraphs through random sampling, making T random selections of n_{sub}-sized sets of nodes. Given N training nodes and T watermarked subgraphs of size n_{sub}, the probability that an attacker-chosen subgraph of size n_{sub} overlaps with any single watermarked subgraph with no less than j nodes is given as:

$$P(\#\text{overlap-nodes} \geq j) = 1 - \left(\sum_{m=1}^{j} \binom{n_{sub}}{m} \binom{N - n_{sub}}{n_{\text{sub}} - m} \Big/ \binom{N}{n_{\text{sub}}} \right)^{T}. \tag{13}$$

The sum is the probability a randomly chosen subgraph and a watermarked subgraph share $< j$ nodes. Raising to power T gives the probability all watermarked subgraphs have $< j$ overlap. 1 minus this value gives the probability that the random subgraph and any watermarked subgraph share $\geq j$ nodes.

5 Experiments

5.1 Setup

Datasets and Training/Testing Sets: We evaluate our watermarking method on four node classification datasets: Amazon Photo (McAuley et al., 2015), CoAuthor CS (Shchur et al., 2019), PubMed (Yang et al., 2016), and Reddit2 (Zeng et al., 2019) (See Appendix A for details). *Our framework can also extend to other graph tasks; see Appendix G.* The graph is split into three sets: 60% for training, 20% for testing, and 20% for further training tasks (e.g., fine-tuning or other robustness evaluations). Training nodes divide into two disjoint sets: one for GNN classifier training, and one consisting of the watermarked subgraphs. (sizes as hyperparameters mentioned below.) The test set is for post-training classification evaluation. The remaining set enables additional training of the pre-trained GNN on unseen data to assess watermark robustness.

GNN Models and Hyperparameters: We apply our watermarking method to four GNN models: GCN Kipf & Welling (2017), SGC (Wu et al., 2019), SAGE (Hamilton et al., 2018), and Graph Transformer (Shi et al., 2020). Our main results use SAGE architecture, and $T = 4$ watermarked subgraphs, each with the size $s = 0.5\%$ of the training nodes.[5] Key hyperparameters in our watermarking method, including the significance levels (α_{tgt} and α_v), balanced hyperparameter (r), and watermark loss contribution bound (ϵ), were tuned to balance classification and watermark losses. A list of all hyperparameter values are in the Appendix. *Note that our watermark design in Equation (11) allows us to learn the watermark length M.*

5.2 Results

As stated in Section 3.3, watermarks should be effective, unique, robust, and undetectable. Our experiments aim to assess each of these. (For more results see Appendix.)

[5]Reddit2 is by far the largest, with 232,965 nodes and 23,213,838 edges. For this reason, only Graph Transformer achieved convergence on Reddit2 in our experiments. Given Reddit's scale, we also default to the smaller $s = 0.03\%$ (46 nodes) for watermarked subgraph size.

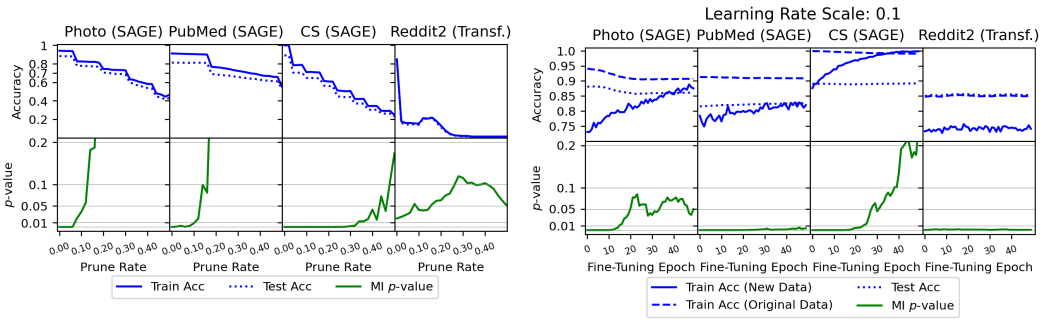

Figure 2: Effect of pruning (left) and fine-tuning (right) on MI p-value, under default settings (GraphSAGE, $T = 4$, $s = 0.005$). See Appendix figures 6-12 for results with varied settings.

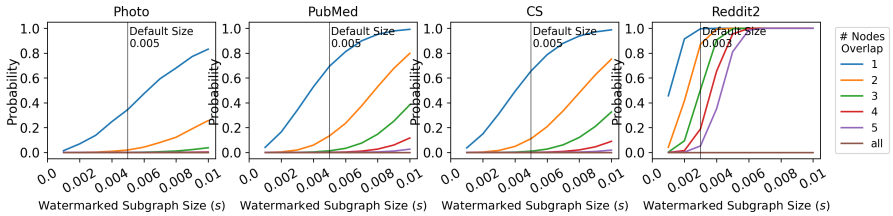

Figure 3: The probability that a randomly-chosen subgraph overlaps with a watermarked subgraph.

5.2.1 Effectiveness and Uniqueness

Embedding *effectiveness* can be measured by the alignment of the binarized explanations with the watermark pattern $\mathbf{w}$ at indices $\mathbf{idx}$; this metric can be used by the owner to confirm that $\mathbf{w}$ was effectively embedded in f during training. Since the entries of $\mathbf{w}$ are 1s and -1s, we simply count the average number of watermarked indices at which a binarized explanation matches $\mathbf{w}$:

$$\textit{Watermark Alignment} = (1/T) \times \Sigma_{i=1}^{T} \Sigma_{j=1}^{M} \mathbb{1}(\hat{\mathbf{e}}_i^{wmk}[\mathbf{idx}[j]] = \mathbf{w}[j]). \tag{14}$$

Watermarking *uniqueness* is measured by the MI p-value for the binarized explanations of the T watermarked subgraphs, as defined by Equation (8). A low p-value indicates the MI is statistically unlikely to be seen in explanations of randomly selected subgraphs. *If the watermarked subgraphs yield a uniquely large MI, it is sufficient, even if alignment is under 100%.*

Table 1 shows results under default settings, averaged over five trials with distinct random seeds and watermark patterns. The MI p-value is below 0.001 for all $T > 2$; this shows *uniqueness* of the ownership claim, meaning the embedding was sufficiently *effective*.

5.2.2 Robustness

We test our method against two types of removal attacks. Pruning compresses models by setting a portion of weights to zero (Li et al., 2016). Following Liu et al. (2021a); Tekgul et al. (2021), we use *structured* pruning, targeting parameter tensor rows and columns based on L_n-norm importance scores (Paszke et al., 2019). Fine-tuning Pan & Yang (2010) adapts already-trained models to a new task (Pan & Yang, 2010) and may make GNNs "forget" watermarks, so it is commonly used for watermark robustness testing Adi et al. (2018); Wang et al. (2020). We test our own method by continuing training on the *validation* dataset, G^{val}, at 0.1 times the original learning rate for 49 epochs. (See Appendix E for results with other learning rates and GNN architectures.)

Figure 2 shows pruning and fine-tuning results. Left: rates of 0.0 (no parameters pruned) to 1.0 (all pruned). In all datasets, the MI p-value only rises as classification accuracy drops, ensuring the owner detects pruning before it impacts the watermark. Right: classification accuracy and MI p-value during fine-tuning. CS has a near-zero MI p-value for 25 epochs; Photo, PubMed and Reddit2 have low MI p-values for the full duration, demonstrating robustness for extended periods of fine-tuning.

We assert that our method also resists data poisoning. Operating on randomly selected subgraphs without data-specific assumptions (unlike backdoor methods), our watermark is embedded post-training-data selection, ensuring immunity to training data changes.

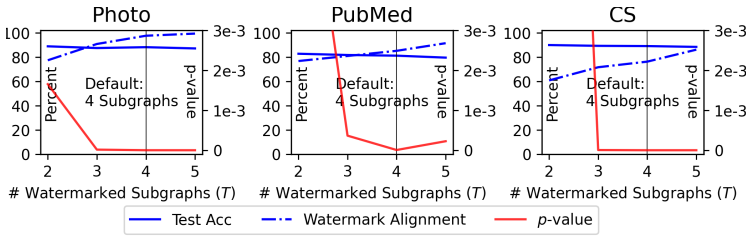

Figure 4: Watermarking metrics for varied T.

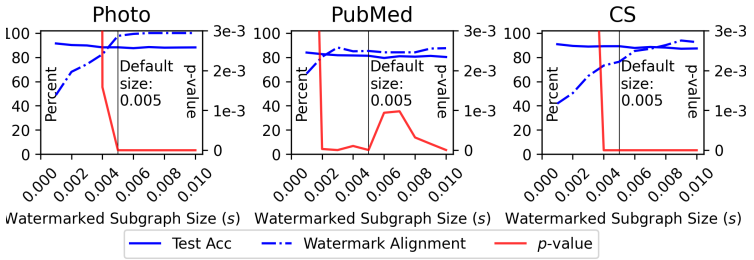

Figure 5: Watermarking metrics for varied s.

5.2.3 Undetectability

Brute-Force Search: With Equations from Section 4.4, we demonstrate the infeasibility of a brute-force search for the watermarked subgraphs in our smallest dataset, Amazon Photo (4590 training nodes). Assume adversaries know the number (T) and size (s) of our watermarked subgraphs. With default $s = 0.005$, each subgraph has $ceil(0.005 \times 4590) = 23$ nodes — there are $\binom{4590}{23} = 6.1 \times 10^{61}$ possible subgraphs; with default $T = 4$, there are $\binom{\binom{4590}{23}}{4} = 5.8 \times 10^{245}$ possible candidate subgraphs, making finding the *uniquely-convincing* set of watermarked subgraphs computationally infeasible.

Random Search: Figure 3 shows probabilities (Equation 13) that a randomly-chosen subgraph's nodes overlap with any watermarked subgraph, for varied sizes s. For $j = 1, \ldots, 5$, or all n_{sub} nodes, probability nears zero that a randomly-selected subgraph overlaps with a common watermarked subgraph by ≥ 3 nodes (given our default watermark subgraph settings $T = 4$ and $s = 0.005$). (The exception is Reddit2, where < 5 nodes is an extremely small portion of the whole dataset.)

5.3 Ablation Studies[6]

Impact of the Number of Watermarked Subgraphs T: Figure 4 shows how T affects watermark performance metrics. For all datasets, larger T increases watermark alignment and a lower p-value, although test accuracy decreases slightly on Photo and PubMed. Notably, the default $T = 4$ is associated with a near-zero p-value in every scenario. Figure 10 in Appendix also shows the robustness results to removal attacks against varied T: we see that the watermarking method resists pruning attacks until test accuracy is affected, and fine-tuning attacks for at least 25 epochs.

Impact of the Size of Watermarked Subgraphs s: Figure 5 shows results with different sizes s. We see similar trends as Figure 4: watermarking is generally more effective, unique, and robust for larger s values. There is again a slight trade-off between subgraph size and test accuracy. For $s \geq 0.003$, our method reaches near-zero p-values for all datasets, as well as increasing watermark alignment. Figure 11 in Appendix shows the robustness results: for all datasets, when $s > 0.005$, our method is robust against pruning attacks generally, and against fine-tuning attacks for at least 25 epochs.

Impact of the Watermark Loss weight r: Table 4 shows the trade-off between the classification accuracy and the watermark effectiveness (suggested by p-value). Empirically, we can still achieve good classification performance while maintaining an effective watermark.

6 Conclusion

We introduce the first GNN watermarking method using explanations, avoiding backdoor-based pitfalls with a statistically unambiguous watermark that resists data attacks. Demonstrating robustness

[6]Note: Reddit2 is excluded from these ablation studies due to computational constraints, as the trends from the other three datasets are sufficient to demonstrate the effects of varying s and T.

against removal attempts and proving the statistical impossibility of locating watermarked subgraphs, our approach significantly advances GNN intellectual property protection.

Reproducibility Statement

Our datasets and implementation details are introduced in Appendix A and the codes are available at https://anonymous.4open.science/r/Explanation_Watermarking_GNN-F6C7.

References

Yossi Adi, Carsten Baum, Moustapha Cisse, Benny Pinkas, and Joseph Keshet. Turning your weakness into a strength: Watermarking deep neural networks by backdooring. In *27th USENIX Security Symposium (USENIX Security 18)*, pp. 1615–1631, 2018.

Arpit Bansal, Ping-yeh Chiang, Michael J Curry, Rajiv Jain, Curtis Wigington, Varun Manjunatha, John P Dickerson, and Tom Goldstein. Certified neural network watermarks with randomized smoothing. In *International Conference on Machine Learning*, pp. 1450–1465. PMLR, 2022.

Huili Chen, Bita Darvish Rouhani, and Farinaz Koushanfar. Blackmarks: Blackbox multibit watermarking for deep neural networks. *ArXiv*, abs/1904.00344, 2018. URL https://api.semanticscholar.org/CorpusID:90260955.

Jialuo Chen, Jingyi Wang, Tinglan Peng, Youcheng Sun, Peng Cheng, Shouling Ji, Xingjun Ma, Bo Li, and Dawn Song. Copy, right? a testing framework for copyright protection of deep learning models. In *2022 IEEE symposium on security and privacy (SP)*, pp. 824–841. IEEE, 2022.

Raphaël Clifford and Alexandru Popa. Maximum subset intersection. *Information Processing Letters*, 111(7): 323–325, 2011. ISSN 0020-0190. doi: https://doi.org/10.1016/j.ipl.2010.12.003. URL https://www.sciencedirect.com/science/article/pii/S0020019010003959.

Bita Darvish Rouhani, Huili Chen, and Farinaz Koushanfar. Deepsigns: An end-to-end watermarking framework for ownership protection of deep neural networks. In *Proceedings of the twenty-fourth international conference on architectural support for programming languages and operating systems*, pp. 485–497, 2019.

Asghar Ghasemi and Saleh Zahediasl. Normality tests for statistical analysis: A guide for non-statisticians. *International Journal of Endocrinology and Metabolism*, 10:486 – 489, 2012. URL https://api.semanticscholar.org/CorpusID:264609266.

Jianping Gou, Baosheng Yu, Stephen Maybank, and Dacheng Tao. Knowledge distillation: A survey, 06 2020.

William L. Hamilton, Rex Ying, and Jure Leskovec. Inductive representation learning on large graphs, 2018. URL https://arxiv.org/abs/1706.02216.

Arthur E. Hoerl and Robert W. Kennard. Ridge regression: Biased estimation for nonorthogonal problems. *Technometrics*, 12(1):55–67, 1970. ISSN 00401706.

Qiang Huang, Makoto Yamada, Yuan Tian, Dinesh Singh, and Yi Chang. Graphlime: Local interpretable model explanations for graph neural networks. *IEEE Transactions on Knowledge and Data Engineering*, 35(7): 6968–6972, 2023. doi: 10.1109/TKDE.2022.3187455.

Thomas N. Kipf and Max Welling. Semi-supervised classification with graph convolutional networks, 2017. URL https://arxiv.org/abs/1609.02907.

Mohammed Lansari, Reda Bellafqira, Katarzyna Kapusta, Vincent Thouvenot, Olivier Bettan, and Gouenou Coatrieux. When federated learning meets watermarking: A comprehensive overview of techniques for intellectual property protection. *Machine Learning and Knowledge Extraction*, 5(4):1382–1406, 2023.

Erwan Le Merrer, Patrick Pérez, and Gilles Trédan. Adversarial frontier stitching for remote neural network watermarking. *Neural Computing and Applications*, 32(13):9233–9244, July 2019. doi: 10.1007/s00521-019-04434-z. URL https://hal.science/hal-02264449.

Bowen Li, Lixin Fan, Hanlin Gu, Jie Li, and Qiang Yang. Fedipr: Ownership verification for federated deep neural network models. *IEEE Transactions on Pattern Analysis and Machine Intelligence*, 45(4):4521–4536, 2022.

Garvin Li. Alibaba cloud machine learning platform for ai: Financial risk control experiment with graph algorithms, 2019. URL https://www.alibabacloud.com/blog/alibaba-cloud-machine-learning-platform-for-ai-financial-risk-%control-experiment-with-graph-algorithms_594518.

Hao Li, Asim Kadav, Igor Durdanovic, Hanan Samet, and Hans Peter Graf. Pruning filters for efficient convnets. *CoRR*, abs/1608.08710, 2016. URL http://arxiv.org/abs/1608.08710.

Hanwen Liu, Zhenyu Weng, and Yuesheng Zhu. Watermarking deep neural networks with greedy residuals. In Marina Meila and Tong Zhang 0001 (eds.), *Proceedings of the 38th International Conference on Machine Learning, ICML 2021, 18-24 July 2021, Virtual Event*, volume 139 of *Proceedings of Machine Learning Research*, pp. 6978–6988. PMLR, 2021a. URL http://proceedings.mlr.press/v139/liu21x.html.

Jian Liu, Rui Zhang, Sebastian Szyller, Kui Ren, and N. Asokan. False claims against model ownership resolution. In *33rd USENIX Security Symposium (USENIX Security 24)*, pp. 6885–6902, Philadelphia, PA, August 2024. USENIX Association. ISBN 978-1-939133-44-1. URL https://www.usenix.org/conference/usenixsecurity24/presentation/liu-jian.

Yang Liu, Xiang Ao, Zidi Qin, Jianfeng Chi, Jinghua Feng, Hao Yang, and Qing He. Pick and choose: a gnn-based imbalanced learning approach for fraud detection. In *Proceedings of the web conference 2021*, pp. 3168–3177, 2021b.

Dongsheng Luo, Wei Cheng, Dongkuan Xu, Wenchao Yu, Bo Zong, Haifeng Chen, and Xiang Zhang. Parameterized explainer for graph neural network. In *Proceedings of the 34th International Conference on Neural Information Processing Systems*, NIPS '20, Red Hook, NY, USA, 2020. Curran Associates Inc. ISBN 9781713829546.

Peizhuo Lv, Pan Li, Shengzhi Zhang, Kai Chen, Ruigang Liang, Hualong Ma, Yue Zhao, and Yingjiu Li. A robustness-assured white-box watermark in neural networks. *IEEE Transactions on Dependable and Secure Computing*, 2023.

Julian J. McAuley, Christopher Targett, Qinfeng Shi, and Anton van den Hengel. Image-based recommendations on styles and substitutes. *CoRR*, abs/1506.04757, 2015. URL http://arxiv.org/abs/1506.04757.

MetaAI. The ai behind unconnected content recommendations on facebook and instagram, 2023. URL https://ai.meta.com/blog/ai-unconnected-content-recommendations-facebook-instagram/.

Luis Perez Oliver Lange. Traffic prediction with advanced graph neural networks, 2020. URL https://deepmind.google/discover/blog/traffic-prediction-with-advanced-graph-neural-networks/.

Sinno Pan and Qiang Yang. A survey on transfer learning. *Knowledge and Data Engineering, IEEE Transactions on*, 22:1345 – 1359, 11 2010. doi: 10.1109/TKDE.2009.191.

Adam Paszke, Sam Gross, Francisco Massa, Adam Lerer, James Bradbury, Gregory Chanan, Trevor Killeen, Zeming Lin, Natalia Gimelshein, Luca Antiga, Alban Desmaison, Andreas Köpf, Edward Z. Yang, Zach DeVito, Martin Raison, Alykhan Tejani, Sasank Chilamkurthy, Benoit Steiner, Lu Fang, Junjie Bai, and Soumith Chintala. Pytorch: An imperative style, high-performance deep learning library. *CoRR*, abs/1912.01703, 2019. URL http://arxiv.org/abs/1912.01703.

Franco Scarselli, Marco Gori, Ah Chung Tsoi, Markus Hagenbuchner, and Gabriele Monfardini. The graph neural network model. *IEEE TNN*, 2008.

Masoumeh Shafieinejad, Nils Lukas, Jiaqi Wang, Xinda Li, and Florian Kerschbaum. On the robustness of backdoor-based watermarking in deep neural networks. In *Proceedings of the 2021 ACM workshop on information hiding and multimedia security*, pp. 177–188, 2021.

Shuo Shao, Wenyuan Yang, Hanlin Gu, Zhan Qin, Lixin Fan, Qiang Yang, and Kui Ren. Fedtracker: Furnishing ownership verification and traceability for federated learning model. *arXiv preprint arXiv:2211.07160*, 2022.

Shuo Shao, Yiming Li, Hongwei Yao, Yiling He, Zhan Qin, and Kui Ren. Explanation as a watermark: Towards harmless and multi-bit model ownership verification via watermarking feature attribution, 2024. URL https://arxiv.org/abs/2405.04825.

Oleksandr Shchur, Maximilian Mumme, Aleksandar Bojchevski, and Stephan Günnemann. Pitfalls of graph neural network evaluation, 2019. URL https://arxiv.org/abs/1811.05868.

Yun Shen, Xinlei He, Yufei Han, and Yang Zhang. Model stealing attacks against inductive graph neural networks, 05 2022.

Yunsheng Shi, Zhengjie Huang, Shikun Feng, Hui Zhong, Wenjin Wang, and Yu Sun. Masked label prediction: Unified message passing model for semi-supervised classification. *arXiv preprint arXiv:2009.03509*, 2020.

Jan Pfeifer Sibon Li, Bryan Perozzi, and Douglas Yarrington. Introducing tensorflow graph neural networks, 2021. URL https://blog.tensorflow.org/2021/11/introducing-tensorflow-gnn.html.

Jacob Steinhardt, Pang Wei Koh, and Percy Liang. Certified defenses for data poisoning attacks. In *Neural Information Processing Systems*, 2017. URL https://api.semanticscholar.org/CorpusID:35426171.

Sebastian Szyller, Buse Gul Atli, Samuel Marchal, and N. Asokan. Dawn: Dynamic adversarial watermarking of neural networks. In *Proceedings of the 29th ACM International Conference on Multimedia*, MM '21, pp. 4417–4425, New York, NY, USA, 2021. Association for Computing Machinery. ISBN 9781450386517. doi: 10.1145/3474085.3475591. URL https://doi.org/10.1145/3474085.3475591.

Buse GA Tekgul, Yuxi Xia, Samuel Marchal, and N Asokan. Waffle: Watermarking in federated learning. In *2021 40th International Symposium on Reliable Distributed Systems (SRDS)*, pp. 310–320. IEEE, 2021.

Yusuke Uchida, Yuki Nagai, Shigeyuki Sakazawa, and Shin'ichi Satoh. Embedding watermarks into deep neural networks. *CoRR*, abs/1701.04082, 2017. URL http://arxiv.org/abs/1701.04082.

Petar Veličković, Guillem Cucurull, Arantxa Casanova, Adriana Romero, Pietro Liò, and Yoshua Bengio. Graph attention networks, 2018. URL https://arxiv.org/abs/1710.10903.

Srinivas Virinchi. Using graph neural networks to recommend related products, 2022. URL https://www.amazon.science/blog/using-graph-neural-networks-to-recommend-related-products.

Asim Waheed, Vasisht Duddu, and N Asokan. Grove: Ownership verification of graph neural networks using embeddings. In *2024 IEEE Symposium on Security and Privacy (SP)*, pp. 2460–2477. IEEE, 2024.

Binghui Wang and Neil Zhenqiang Gong. Attacking graph-based classification via manipulating the graph structure. In *Proceedings of the 2019 ACM SIGSAC Conference on Computer and Communications Security*, pp. 2023–2040, 2019.

Jiangfeng Wang, Hanzhou Wu, Xinpeng Zhang, and Yuwei Yao. Watermarking in deep neural networks via error back-propagation. *Electronic Imaging*, 2020:22–1, 01 2020. doi: 10.2352/ISSN.2470-1173.2020.4.MWSF-022.

Siyue Wang, Xiao Wang, Pin-Yu Chen, Pu Zhao, and Xue Lin. High-robustness, low-transferability fingerprinting of neural networks. *arXiv preprint arXiv:2105.07078*, 2021.

Tianhao Wang and Florian Kerschbaum. Riga: Covert and robust white-box watermarking of deep neural networks. *Proceedings of the Web Conference 2021*, 2020. URL https://api.semanticscholar.org/CorpusID:225062005.

Mitchell Wortsman, Gabriel Ilharco, Saurabh S. Gadre, Rebecca Roelofs, Raphael Gontijo-Lopes, Ari S. Morcos, Hongseok Namkoong, Ali Farhadi, Yair Carmon, Simon Kornblith, and Ludwig Schmidt. Model soups: Averaging weights of multiple fine-tuned models improves accuracy without increasing inference time. In *Proceedings of the International Conference on Machine Learning*, ICML '22, pp. 23965–23998. PMLR, June 2022.

Felix Wu, Amauri Souza, Tianyi Zhang, Christopher Fifty, Tao Yu, and Kilian Weinberger. Simplifying graph convolutional networks. In Kamalika Chaudhuri and Ruslan Salakhutdinov (eds.), *Proceedings of the 36th International Conference on Machine Learning*, volume 97 of *Proceedings of Machine Learning Research*, pp. 6861–6871. PMLR, 09–15 Jun 2019. URL https://proceedings.mlr.press/v97/wu19e.html.

Jing Xu, Stefanos Koffas, Oğuzhan Ersoy, and Stjepan Picek. Watermarking graph neural networks based on backdoor attacks. In *2023 IEEE 8th European Symposium on Security and Privacy (EuroS&P)*, pp. 1179–1197. IEEE, 2023.

Makoto Yamada, Wittawat Jitkrittum, Leonid Sigal, Eric P. Xing, and Masashi Sugiyama. High-dimensional feature selection by feature-wise kernelized lasso. *Neural Computation*, 26:185–207, 2012. URL https://api.semanticscholar.org/CorpusID:2742785.

Yifan Yan, Xudong Pan, Mi Zhang, and Min Yang. Rethinking {White-Box} watermarks on deep learning models under neural structural obfuscation. In *32nd USENIX Security Symposium (USENIX Security 23)*, pp. 2347–2364, 2023.

Hongxia Yang. Aligraph: A comprehensive graph neural network platform. In *ACM SIGKDD international conference on knowledge discovery & data mining*, pp. 3165–3166, 2019.

Zhilin Yang, William W. Cohen, and Ruslan Salakhutdinov. Revisiting semi-supervised learning with graph embeddings, 2016. URL https://arxiv.org/abs/1603.08861.

Rex Ying, Dylan Bourgeois, Jiaxuan You, Marinka Zitnik, and Jure Leskovec. Gnnexplainer: Generating explanations for graph neural networks. In *Proceedings of the 33rd International Conference on Neural Information Processing Systems*, 2019.

Hanqing Zeng, Hongkuan Zhou, Ajitesh Srivastava, Rajgopal Kannan, and Viktor Prasanna. Graphsaint: Graph sampling based inductive learning method. *arXiv preprint arXiv:1907.04931*, 2019.

Hengtong Zhang, T. Zheng, Jing Gao, Chenglin Miao, Lu Su, Yaliang Li, and Kui Ren. Data poisoning attack against knowledge graph embedding. In *International Joint Conference on Artificial Intelligence*, 2019. URL https://api.semanticscholar.org/CorpusID:195345427.

Jialong Zhang, Zhongshu Gu, Jiyong Jang, Hui Wu, Marc Ph. Stoecklin, Heqing Huang, and Ian Molloy. Protecting intellectual property of deep neural networks with watermarking. *Proceedings of the 2018 on Asia Conference on Computer and Communications Security*, 2018. URL https://api.semanticscholar.org/CorpusID:44085059.

Xiao-Meng Zhang, Li Liang, Lin Liu, and Ming-Jing Tang. Graph neural networks and their current applications in bioinformatics. *Frontiers in Genetics*, 12, 2021. ISSN 1664-8021. doi: 10.3389/fgene.2021.690049. URL https://www.frontiersin.org/articles/10.3389/fgene.2021.690049.

Jie Zhou, Ganqu Cui, Shengding Hu, Zhengyan Zhang, Cheng Yang, Zhiyuan Liu, Lifeng Wang, Changcheng Li, and Maosong Sun. Graph neural networks: A review of methods and applications. *AI Open*, 1:57–81, 2020. ISSN 2666-6510. doi: https://doi.org/10.1016/j.aiopen.2021.01.001. URL https://www.sciencedirect.com/science/article/pii/S2666651021000012.

Yuchen Zhou, Hongtao Huo, Zhiwen Hou, and Fanliang Bu. A deep graph convolutional neural network architecture for graph classification. *PLOS ONE*, 18, 2023. URL https://api.semanticscholar.org/CorpusID:257428249.

Daniel Zügner, Oliver Borchert, Amir Akbarnejad, and Stephan Günnemann. Adversarial attacks on graph neural networks: Perturbations and their patterns. *ACM Trans. Knowl. Discov. Data*, 14(5), jun 2020. ISSN 1556-4681. URL https://doi.org/10.1145/3394520.

APPENDIX

A EXPERIMENTAL SETUP DETAILS

Hardware and Software Specifications. All experiments were conducted on a MacBook Pro (Model Identifier: MacBookPro18,3; Model Number: MKGR3LL/A) with an Apple M1 Pro chip (8 cores: 6 performance, 2 efficiency) and 16 GB of memory, on macOS Sonoma Version 14.5. Models were implemented in Python with the PyTorch framework.

Dataset Details. Amazon Photo (simply "Photo" in this paper) is a subset of the Amazon co-purchase network (McAuley et al., 2015). Nodes are products, edges connect items often purchased together, node features are bag-of-words product reviews, and class labels are product categories. Photo has 7,650 nodes, 238,163 edges, 745 node features, and 8 classes. The CoAuthor CS dataset ("CS" in this paper) (Shchur et al., 2019) is a graph whose nodes are authors, edges are coauthorship, node features are keywords, and class labels are the most active fields of study by those authors. CS has 18,333 nodes, 163,788 edges, 6,805 node features, and 15 classes. Lastly, PubMed (Yang et al., 2016) is a citation network whose nodes are documents, edges are citation links, node features are TF-IDF weighted word vectors based on the abstracts of the papers, and class labels are research fields. The graph has 19,717 nodes, 88,648 edges, 500 features, and 3 classes. Reddit2 (Zeng et al., 2019) is a large social network where nodes represent posts, edges connect posts if the same user commented on both, node features are post embeddings, and class labels are communities. It contains 232,965 nodes, 114,848,857 edges, 602 features, and 41 classes.

Hyperparameter Setting Details.

Classification training hyperparameters:

- Learning rate: 0.001-0.001
- Number of layers: 3
- Hidden Dimensions: 256-512
- Epochs: 100-300

Watermarking hyperparameters:

- Target significance level, α_{tgt}: set to 1e-5 to ensure a watermark size that is sufficiently large.
- Verification significance level, α_v: set to 0.01 to limit false verifications to under 1% likelihood.
- Watermark loss coefficient, r: set to values between 20-100, depending on the amount required to bring L^{wmk} to a similar scale as L^{clf} to ensure balanced learning.
- Watermark loss parameter ϵ: set to values ranging from 0.01 to 0.1. Smaller values ensure that no watermarked node feature index has undue influence on watermark loss.

B GAUSSIAN KERNEL MATRICES

Define $\bar{\boldsymbol{K}}$ as a collection of matrices $\{\bar{\boldsymbol{K}}^{(1)}, \ldots, \bar{\boldsymbol{K}}^{(F)}\}$, where $\bar{\boldsymbol{K}}^{(k)}$ (size $N \times N$) is the centered and normalized version of Gaussian kernel matrix $\boldsymbol{K}^{(k)}$, and each element $\boldsymbol{K}_{uv}^{(k)}$ is the output of the Gaussian kernel function on the k^{th} node feature for nodes u and v:

$$\bar{\boldsymbol{K}}^{(k)} = \boldsymbol{H}\boldsymbol{K}^{(k)}\boldsymbol{H}/\|\boldsymbol{H}\boldsymbol{K}^{(k)}\boldsymbol{H}\|_F,\ \boldsymbol{H} = \boldsymbol{I}_N - \frac{1}{N}\mathbf{1}_N\mathbf{1}_N^T,\ \boldsymbol{K}_{uv}^{(k)} = \exp\left(-\frac{1}{2\sigma_x^2}\left(\mathbf{x}_u^{(k)} - \mathbf{x}_v^{(k)}\right)^2\right). \tag{15}$$

$\|\cdot\|_F$ is the Frobenius norm, $\boldsymbol{H}$ is a centering matrix (where $\boldsymbol{I}_N$ is an $N \times N$ identity matrix and $\mathbf{1}_N$ is an all-one vector of length N), and σ_x is Gaussian kernel width. Now take the nodes' softmax scores $\mathbf{P} = [\mathbf{p}_1, \cdots, \mathbf{p}_N]$, and their Guassian kernel width, $\sigma_{\mathbf{p}}$. Define $\bar{\boldsymbol{L}}$ as a centered and normalized $N \times N$ Gaussian kernel $\boldsymbol{L}$, where $\boldsymbol{L}_{uv}$ is the similarity between nodes u and v's softmax outputs:

$$\bar{\boldsymbol{L}} = \boldsymbol{H}\boldsymbol{L}\boldsymbol{H}/\|\boldsymbol{H}\boldsymbol{L}\boldsymbol{H}\|_F, \quad \boldsymbol{L}_{uv} = \exp\left(-\frac{1}{2\sigma_{\mathbf{p}}^2}\|\mathbf{p}_u - \mathbf{p}_v\|_2^2\right). \tag{16}$$

Let $\tilde{\boldsymbol{K}}$ be the $N^2 \times F$ matrix $[\mathrm{vec}(\bar{\boldsymbol{K}}^{(1)}), \ldots, \mathrm{vec}(\bar{\boldsymbol{K}}^{(F)})]$, where $\mathrm{vec}(\cdot)$ converts each $N \times N$ matrix $\bar{\boldsymbol{K}}^{(k)}$ into a N^2-dimensional column vector. Similarly, we denote $\tilde{\boldsymbol{L}} = \mathrm{vec}(\bar{\boldsymbol{L}})$ as the N^2-dimensional, vector form of the matrix $\bar{\boldsymbol{L}}$. Also take $F \times F$ identity matrix $\boldsymbol{I}_F$ and regularization hyperparameter λ.

Algorithm 1: Watermark Embedding

Input: Graph G, training nodes $\mathcal{V}^{tr}$, learning rate η, #watermarked subgraphs T, watermarked subgraph size s, hyperparameter r, target significance α_{tgt}, watermark loss contribution bound ϵ.

Output: A trained and watermarked model, f.

Setup: Initialize f and optimizer. With α_{tgt}, T, and number of node features F as input, compute M using equation 11. Initialize $\mathbf{w}$ with values 1 and -1 uniform at random. With $n_{sub} = ceil(s \times |\mathcal{V}^{tr}|)$, randomly sample T sets of n_{sub} nodes from $\mathcal{V}^{tr}$. These subgraphs jointly comprise G^{wmk}. Define node set $\mathcal{V}^{clf}$ for classification from the remaining nodes in $\mathcal{V}^{tr}$.

for epoch=1 to #Epoch **do**
  $L^{clf} \leftarrow \mathcal{L}_{CE}(\mathbf{y}^{clf}, f_\Theta(\mathcal{V}^{clf}))$
  $L^{wmk} \leftarrow 0$
  for i=1 to T **do**
    $\mathbf{P}_i^{wmk} \leftarrow f_\Theta(\mathcal{V}_i^{wmk})$
    $\mathbf{e}_i^{wmk} \leftarrow explain(\mathbf{X}_i^{wmk}, \mathbf{P}_i^{wmk})$
    $L^{wmk} \leftarrow L^{wmk} + \sum_{j=1}^{M} \max(0, \epsilon - \mathbf{w}[j] \cdot \mathbf{e}_i^{wmk}[\mathbf{idx}[j]])$
  end
  $L \leftarrow L^{clf} + r \cdot L^{wmk}$
  $\Theta \leftarrow \Theta - \eta \frac{\partial L}{\partial \Theta}$
end

C Time Complexity Analysis

The training process involves optimizing for node classification and embedding the watermark. To obtain total complexity, we therefore need to consider two processes: forward passes with the GNN, and explaining the watermarked subgraphs.

GNN Forward Pass Complexity. The complexity of standard node classification in GNNs comes from two main processes: message passing across edges ($O(EF)$, where E is number of edges and F is number of node features), and weight multiplication for feature transformation ($O(NF^2)$, where N is number of nodes). For L layers, the time complexity of a forward pass is therefore:

$$O(L(EF + NF^2))$$

Explanation Complexity. Consider the Formula 3 for computing the explanation: $\mathbf{e} = explain(\mathbf{X}, \mathbf{P}) = (\tilde{\boldsymbol{K}}^T \tilde{\boldsymbol{K}} + \lambda \boldsymbol{I}_F)^{-1} \tilde{\boldsymbol{K}}^T \tilde{\boldsymbol{L}}$. Remember that $\tilde{\boldsymbol{K}}$ is an $N^2 \times F$ matrix, I_F is a $F \times F$ matrix, and $\tilde{\boldsymbol{L}}$ is a $N^2 \times 1$ vector. To compute the complexity of this computation, we need the complexity of each subsequent order of operations:

1. Multiplying $\tilde{\boldsymbol{K}}^T \tilde{\boldsymbol{K}}$ (an $O(F^2N^2)$ operation, resulting in an $F \times F$ matrix)
2. Obtaining and adding $\lambda \boldsymbol{I}_F$ (an $O(F^2)$ operation, resulting in an $F \times F$ matrix)
3. Inverting the result (an $O(F^3)$ operation, resulting in an $F \times F$ matrix)
4. Multiplying by $\tilde{\boldsymbol{K}}^T$ (an $O(F^2N^2)$ operation, resulting in an $F \times N^2$ matrix)
5. Multiplying the result by $\tilde{\boldsymbol{L}}$ (an $O(F^2N^2)$ operation, resulting in an $N^2 \times 1$ vector)

The total complexity of a single explanation is therefore $O(F^2N^2) + O(F^2) + O(F^3) + O(F^2N^2) + O(F^2N^2) = O(F^2N^2 + F^3)$. For obtaining explanations of T subgraphs during a given epoch of watermark embedding, the complexity is therefore:

$$O(T(F^2N^2 + F^3))$$

Total Complexity. The total time complexity over i epochs is therefore:

$$O\left(i \times \left(L(EF + NF^2) + T(F^2N^2 + F^3)\right)\right)$$

The above calculation is based on general graph notations in Section 3.1. The actual explanation complexity is much smaller. For the ridge regression, as mentioned in Section 4.1, we use only the nodes from the subgraphs

Algorithm 2: Ownership Verification

Input: A GNN f trained by Alg. 1, a graph G with training nodes $\mathcal{V}^{tr}$, a collection of T *candidate subgraphs* with node size n_{sub}, and a significance level α_v required for verification, I iterations.
Output: Ownership verdict.

Phase 1 – Obtain distribution of naturally-occurring matches

Setup:

1. Define subgraphs $\mathcal{S} = \{G_1^{rand}, \cdots, G_D^{rand}\}$, where each subgraph is size $n_{sub} = ceil(s \times |\mathcal{V}^{tr}|)$. Each subgraph G_i^{rand} is defined by randomly selecting n_{sub} nodes from $\mathcal{V}^{tr}$. D should be "sufficiently large" ($D > 100$) to approximate a population.
2. Using Equation 6, collect *binarized explanations*, $\hat{\mathbf{e}}_i^{rand}$, for $1 \le i \le D$.
3. Initialize empty list, $matchCounts = \{\}$.

for i=1 to I simulations **do**

Randomly select T distinct indices $idx_1, \ldots, idx_T$ from the range $\{1, \cdots, D\}$.
For each idx_i, let $\mathcal{V}_{idx_i}^{rand}$ and $\mathbf{X}_{idx_i}^{rand}$ be the nodes of $G_{idx_i}^{rand}$ and their features, respectively.
Compute $\hat{\mathbf{e}}_{idx_i}^{rand} = sign(explain(\mathbf{X}_{idx_i}^{rand}, f(\mathcal{V}_{idx_i}^{rand}))$ for each i in $1 \le i \le T$.
Compute the MI on $\{\hat{\mathbf{e}}_{idx_1}^{rand}, \cdots, \hat{\mathbf{e}}_{idx_T}^{rand}\}$ using Equation 7, and append to $matchCounts$.

Compute $\mu_{nat_e} = \frac{\Sigma_{i=1}^{I} matchCounts[i]}{I}$ and $\sigma_{nat_e} = \sqrt{\frac{1}{I}\Sigma_{i=1}^{I}(matchCounts[i] - \mu_{nat_e})^2}$.

Phase 2 – Significance testing

Consider the null hypothesis, H_0, that the observed MI across T binarized explanations in $\{\hat{\mathbf{e}}_i^{cdt}\}_{i=1}^{T}$ comes from the population of naturally-occurring matches. We conduct a z-test to test H_0:

1. For $1 \le i \le T$, let $\mathbf{P}_i^{cdt} = f(\mathcal{V}_i^{cdt})$ and $\mathbf{X}_i^{cdt}$ be the corresponding features of $\mathcal{V}_i^{cdt}$.
2. Let the binarized explanation of the i^{th} candidate subgraph be defined as:

$$\hat{\mathbf{e}}_i^{cdt} = sign\left(explain(\mathbf{X}_i^{cdt}, \mathbf{P}_i^{cdt})\right)$$

3. Compute MI^{cdt} across tensors in $\{\hat{\mathbf{e}}_i^{cdt}\}_{i=1}^{T}$ using Equation 14.
4. Compute the significance of this value as the p-value of a one-tailed z-test:

$$z_{test} = \frac{\text{MI}^{cdt} - \mu_{nat_e}}{\sigma_{nat_e}} \qquad p_{z_{test}} = 1 - \Phi(z_{test}),$$

Where $\Phi(z_{test})$ is the cumulative distribution function of the standard normal distribution.

5. If $p_{z_{test}} \ge \alpha_v$, the candidate subgraphs *do not* provide adequate ownership evidence. If $p_{z_{test}} < \alpha_v$, the candidate subgraphs provide enough evidence of ownership to reject H_0.

$\{G_1^{wmk}, \ldots, G_T^{wmk}\}$. Here, N is the number of nodes in $\{G_1^{wmk}, \ldots, G_T^{wmk}\}$. Additionally, as mentioned in Section 4.3, the original feature space of size F is masked to a subset of size M, which reduces the complexity of backpropagating the watermark loss.

Training Duration (Wall Time). We evaluate the training duration on the Photo and PubMed datasets under both watermarked and non-watermarked settings. The corresponding training times are reported in Table 2. In both cases, the models are trained using 7 subgraphs. The architecture comprises three layers with a hidden dimension of 256. The results suggest that introducing the watermark does not increase the training time to a prohibitive degree.

Table 2: Model Training time (in seconds) with and without watermarking.

Dataset	Architecture	Epochs	Without Watermark (s)	With Watermark (s)
Photo	GCN	300	91.72	147.25
Photo	SAGE	300	109.06	167.28
PubMed	GCN	200	59.20	96.84
PubMed	SAGE	200	65.18	98.98

D Normality of Matching Indices Distribution

Our results rely on the z-test to demonstrate the significance of the MI metric. To confirm that this test is appropriate, we need to demonstrate that the MI values follow a normal distribution. Table 3 shows the results of applying the Shapiro-Wilk Ghasemi & Zahediasl (2012) normality test to MI distributions obtained under different GNN architectures and datasets. The results show p-values significantly above 0.1, indicating we cannot reject the null hypothesis of normality.

Table 3: Shapiro-Wilk Test p-values

Dataset	SAGE	SGC	GCN
Photo	0.324	0.256	0.345
CS	0.249	0.240	0.205
PubMed	0.249	0.227	0.265

E Additional Results

Tradeoff between classification performance and watermark effectiveness. As mentioned in Section 5.3, we observe a trade-off between the classification accuracy and the watermark effectiveness. Here, we include the corresponding empirical results. r represents the weight of the watermark loss.

Table 4: Effect of r on accuracy and MI p-value across datasets.

Dataset	r	Accuracy (Train/Valid/Test)	p-value
Photo	0	0.957 / 0.937 / 0.948	–
Photo	1	0.955 / 0.937 / 0.950	0.23
Photo	20	0.951 / 0.937 / 0.946	0.012
Photo	100	0.937 / 0.934 / 0.939	1.00×10^{-4}
Photo	200	0.928 / 0.933 / 0.931	0.002
PubMed	0	0.899 / 0.876 / 0.871	–
PubMed	1	0.894 / 0.876 / 0.865	4.67×10^{-6}
PubMed	20	0.874 / 0.867 / 0.860	0
PubMed	100	0.813 / 0.811 / 0.806	0
PubMed	200	0.730 / 0.723 / 0.735	0

Fine-tuning and pruning under more GNN architectures. The main paper mainly show results on GraphSAGE (Hamilton et al., 2018). Here, we also explore GCN Kipf & Welling (2017) and SGC (Wu et al., 2019). Figure 6-Figure 9 shows the impact of fine-tuning and pruning attacks results on our watermarking method under these two architectures. Watermarked GCN and SGC models fared well against fine-tuning attacks for the Photo and CS datasets, but less so for PubMed; meanwhile, these models were robust against pruning attacks for Pubmed and CS datasets, but not Photo. Since the owner can assess performance against these removal attacks prior to deploying their model, they can simply a matter of training each type as effectively as possible and choosing the best option. In our case, GraphSAGE fared best for our three datasets, but GCN and SGC were viable solutions in some cases.

More Results on Effectiveness and Uniqueness. Table 1 in the main paper shows the test accuracy, watermark alignment, and MI p-values of our experiments with the default value of $T = 4$. In Table 5, we additionally

Table 5: Watermarking results for varied T. Each value averages 5 trials with distinct random seeds.

		Number of Subgraphs (T)											
		2			3			4			5		
Dataset	GNN	Acc (Trn/Tst)	Wmk Align	MI p-val	Acc (Trn/Tst)	Wmk Align	MI p-val	Acc (Trn/Tst)	Wmk Align	MI p-val	Acc (Trn/Tst)	Wmk Align	MI p-val
Photo	GCN	92.5/89.7	73.0	0.087	91.5/88.9	86.1	<0.001	90.9/88.3	91.4	<0.001	90.6/88.2	95.2	<0.001
	SGC	92.0/89.4	73.8	0.111	91.0/88.7	82.5	<0.001	90.1/88.0	91.8	<0.001	89.7/87.4	99.4	<0.001
	SAGE	95.4/88.9	77.4	0.002	94.4/87.5	90.9	<0.001	94.1/88.2	97.7	<0.001	93.9/87.2	99.4	<0.001
PubMed	GCN	87.0/83.7	75.4	0.003	85.9/82.1	86.6	<0.001	85.7/81.4	91.5	<0.001	85.6/81.4	90.2	<0.001
	SGC	86.7/83.1	79.7	<0.001	85.8/81.6	83.8	<0.001	85.3/81.4	88.9	<0.001	84.6/80.0	92.9	<0.001
	SAGE	91.9/82.8	76.8	0.009	91.3/81.8	81.0	<0.001	91.1/81.2	85.2	<0.001	90.1/79.6	91.5	<0.001
CS	GCN	97.1/90.3	56.8	0.562	96.8/89.9	67.5	<0.001	96.8/89.8	73.8	<0.001	96.9/90.0	78.9	<0.001
	SGC	97.2/90.3	57.1	0.003	96.8/89.9	67.7	<0.001	96.7/90.1	74.5	<0.001	96.6/89.8	77.8	<0.001
	SAGE	99.9/90.2	61.5	0.233	99.9/89.4	73.3	<0.001	99.9/88.9	78.2	<0.001	99.9/88.3	84.0	<0.001

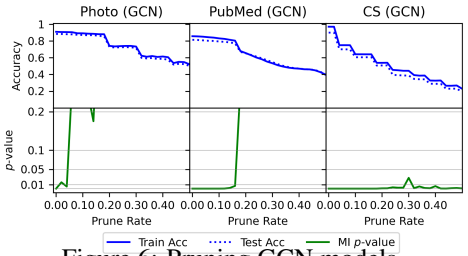

Figure 6: Pruning GCN models.

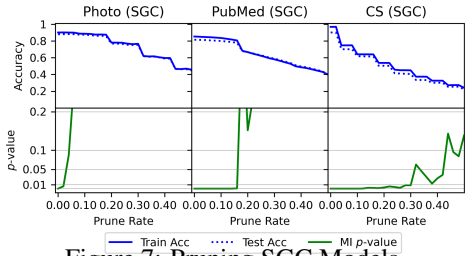

Figure 7: Pruning SGC Models.

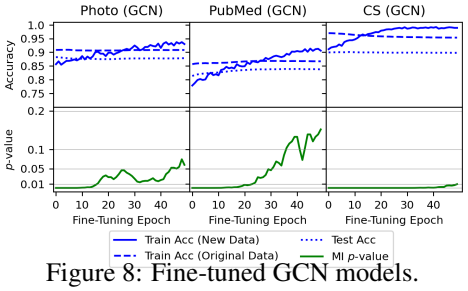

Figure 8: Fine-tuned GCN models.

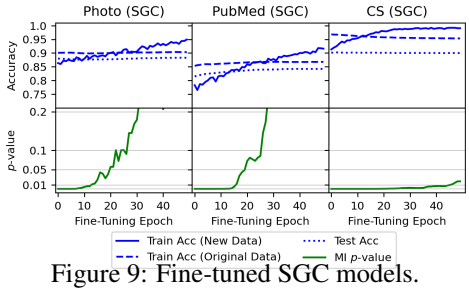

Figure 9: Fine-tuned SGC models.

present the results for $T = 2$, $T = 3$, and $T = 5$. The results show MI p-values below 0.001 across all configurations when $T \geq 3$. They also show increasing watermark alignment with increasing T, however, with a slight trade-off in classification accuracy: when increasing from $T = 2$ to $T = 5$, watermark alignment increases, but train and test classification accuracy decreases by an average of 1.44% and 2.13%, respectively; despite this, both train and test classification accuracy are generally high across all datasets and models.

Fine-Tuning and Pruning under varied watermark sizes. Figures 10 and 11 show the robustness of our methods to fine-tuning and pruning removal attacks when T and s are varied. We observe that, for $T \geq 4$ and $s \geq 0.005$ — our default values — pruning only affects MI p-value after classification accuracy has already been affected; at this point the pruning attack would be detected by model owners regardless. Similarly, across all datasets, for $T \geq 4$ and $s \geq 0.005$, our method demonstrates robustness against the fine-tuning attack for at least 25 epochs.

Fine-Tuning under varied learning rates. Our main fine-tuning results (see Figure **??**) scale the learning rate to 0.1 times its original training value. Figure 12 additionally shows results for learning rates scaled to 1× and 10× the original training rates. The results for scaling the learning rate by 1× show that larger learning rates quickly remove the watermark. However, these figures also demonstrate that, by the time training accuracy on the fine-tuning dataset has reached an acceptable level of accuracy, the accuracy on the original training set drops significantly, which diminishes the usefulness of the fine-tuned model on the original task. For larger rates (10×), the watermark is removed almost immediately, but the learning trends and overall utility of the model are so unstable that the model is rendered useless. Given this new information, our default choice to fine-tune at 0.1× the original learning rate is the most reasonable scenario to consider.

Watermark effectiveness after model merge. Model merge is a common strategy to merge two models that share the optimization trajectory. We conduct experiments that show the robustness of the watermark after the model merge. Following the idea in (Wortsman et al., 2022), we generate a new model by averaging parameters

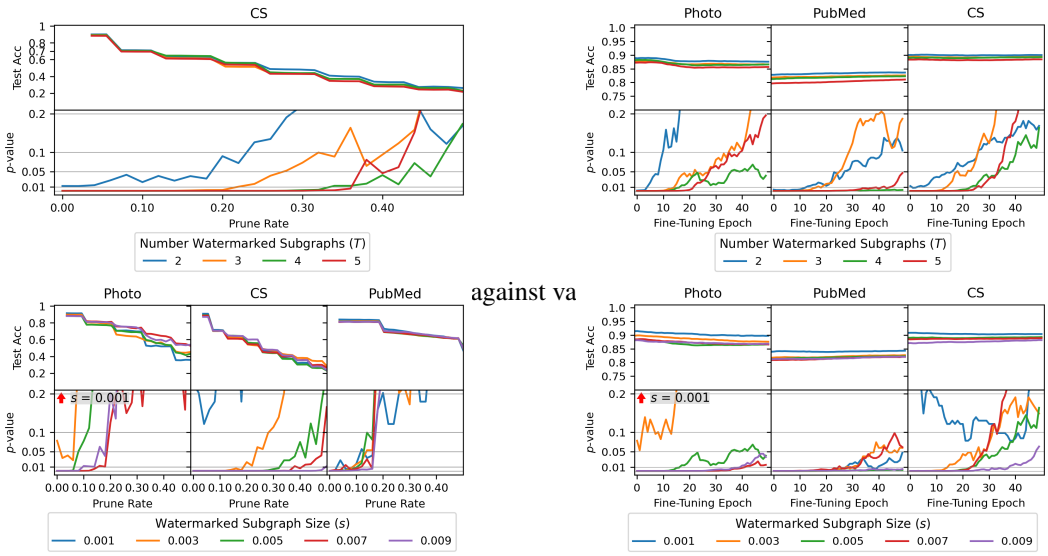

against va

Figure 11: Pruning and fine-tuning attacks against varied sizes of watermarked subgraphs (s)

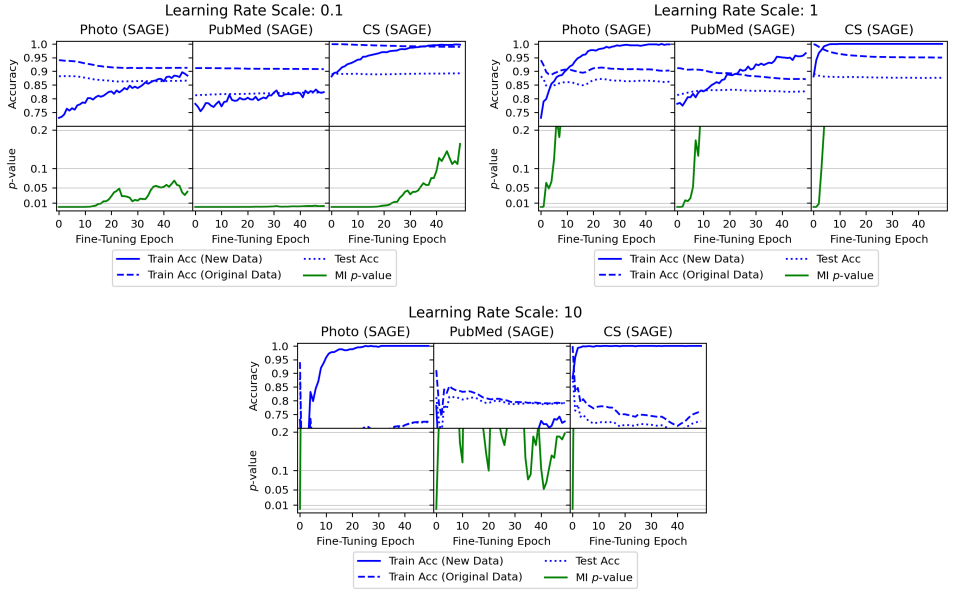

Figure 12: Fine-tuning results at increased learning rates (SAGE architecture).

from the watermark model and the fine-tuned watermark model. Table 6 shows effective watermark (suggested by p-value) in the merged model.

F KNOWLEDGE DISTILLATION ATTACK

An important future direction is to safeguard our method against model extraction attacks Shen et al. (2022), which threaten to steal a model's functionality without preserving the watermark. One form of model extraction attack is knowledge distillation attack Gou et al. (2020).

Knowledge distillation has two models: the original "teacher" model, and an untrained "student" model. During each epoch, the student model is trained on two objectives: (1) correctly classify the provided input, and (2) mimic the teacher model by mapping inputs to the teacher's predictions. The student therefore learns to map inputs to the teacher's "soft label" outputs (probability distributions)

Table 6: Accuracy of the Watermarked and Merged Models and the MI p-value of the Merged Model

Architecture	Watermark Model Acc. (train/valid/test)	Merged Model Acc. (train/valid/test)	p-value
GCN	0.862/0.807/0.801	0.861/0.816/0.813	9.633e-7
SAGE	0.905/0.790/0.776	0.897/0.801/0.786	0.007
Transformer	0.904/0.790/0.782	0.906/0.798/0.790	0.008

alongside the original hard labels; this guided learning process leverages the richer information in the teacher's soft label outputs, which capture nuanced relationships between classes that hard labels cannot provide. By focusing on these relationships, the student model can generalize more efficiently and achieve comparable performance to the teacher with a smaller model and fewer parameters, thus reducing complexity.

We find that in the absence of a strategically-designed defense, the knowledge distillation attack successfully removes our watermark ($p > 0.05$). This is unsurprising, since model distillation maps inputs to outputs but ignores mechanisms that lead to auxiliary tasks like watermarking.

To counter this, we outline a defense mechanism that would incorporate watermark robustness to knowledge distillation. This method strategically injects the watermark pattern directly into the teacher model's soft-label output space during the distillation phase, thereby enforcing its mandatory inheritance by the student model.

Watermark Vector Generation. The mechanism begins by generating a highly structured perturbation vector ($\mathbf{v}$) for each input graph, where the dimensionality matches the number of classification classes (C). The perturbation vector $\mathbf{v}$ is constructed via a linear transformation involving two private components: (1) Gaussian projection matrix ($\mathbf{A}$): A randomly generated matrix $\mathbf{A} \in \mathbb{R}^{C \times M}$ sampled from a Gaussian Distribution. (2) The watermark ground truth ($\mathbf{w}$): The watermark pattern $\mathbf{w} \in \mathbb{R}^{M}$, where M is the length of watermark. The perturbation vector is computed as:

$$\mathbf{v} = \mathbf{A}\mathbf{w}$$

Logits Perturbation and Normalization. The perturbation vector $\mathbf{v}$, whose dimension C matches the logits space, is then normalized by using L_2 normalization to ensure its magnitude is minute. This normalization step is crucial for achieving utility preservation. The normalized vector $\mathbf{v}'$ is then added to the teacher model's original logits ($\mathbf{z}_T$) for each node:

$$\mathbf{z}'_T = \mathbf{z}_T + \mathbf{v}'$$

Knowledge Distillation Enforcement. All the steps above are performed before the KD process. During the KD process, the student model is forced to minimize the Kullback-Leibler (KL) divergence between its own soft-label predictions ($\mathbf{P}_S$) and the perturbed soft-label predictions ($\mathbf{P}'_T$) derived from $\mathbf{Z}'_T$.

$$\mathcal{L}_{KD} = T^2 \cdot \mathrm{KL}\left(\mathrm{LogSoftmax}\left(\frac{\mathbf{z}_S}{T}\right) \| \mathrm{Softmax}\left(\frac{\mathbf{z}'_T}{T}\right)\right)$$

Because the $\mathbf{v}'$ vector is numerically negligible after normalization, adding it to the logits causes no significant degradation (i.e., minimal utility loss) to the teacher's classification accuracy. However, $\mathbf{v}'$ contains the secret linear structure defined by $\mathbf{A}$ and $\mathbf{w}$.

The student model, in its attempt to precisely mimic the rich information in the perturbed soft labels ($\mathbf{P}'_T$), is consequently forced to inherit the linear relationship defined by the secret watermark pattern $\mathbf{w}$, thereby achieving Transferable Watermarking.

Verification and Evaluation. Here, we evaluate the effectiveness of this mechanism against Knowledge Distillation (KD) attacks. The results on the Photo dataset using the GCN architecture can be found in Table 7. It demonstrates that our watermark exhibits robust transferability to the student model. The student model maintained high classification accuracy on the task, confirming that the normalized logits perturbation ($\mathbf{v}'$) did not significantly compromise the model's primary utility. The measured Matching Index (MI) for the watermarked subgraphs yielded a low P-value (P

≤ 0.05), achieving the required statistical significance for ownership verification. This confirms that the watermark pattern was successfully inherited and preserved within the student model's feature attribution space despite the model compression achieved through KD.

Table 7: Experimental Validation of Robust Watermark Transfer under Knowledge Distillation Attack.

# Subgraph Collections	6		7	
	without	**with**	without	**with**
p-value	0.352	**0.037**	0.225	**0.025**
Acc (train/test)	0.904/0.883	**0.904/0.880**	0.904/0.881	**0.903/0.880**

G Future Directions

While we have primarily provided results for the node-classification case, we believe much of our logic can be extended to other graph learning tasks, including edge classification and graph classification. Our method embeds the watermark into explanations of predictions on various graph features. Specifically, for node predictions, we obtain feature attribution vectors for the $n \times F$ node feature matrices of T target subgraphs, with a loss function that penalizes deviations from the watermark. This process can be adapted to link prediction and graph classification tasks as long as we can derive T separate $n \times F$ feature matrices, where n represents the number of samples per group and F corresponds to the number of features for the given data structure (e.g., node, edge, or graph). Below, we outline how this extension applies to different classification tasks:

1. **Node Classification:** The dataset is a single graph. Subgraphs are formed by randomly selecting $n = s \cdot |\mathcal{V}^{tr}|$ nodes from the training set (where $|\mathcal{V}^{tr}|$ is the number of training nodes and s is a proportion of that size). (Note: in this case, n is equal to the value n_{sub} referenced previously in the paper.) For each subgraph:
   - The $n \times F$ node feature matrix represents the input features (F is the number of node features).
   - The $n \times 1$ prediction vector contains one label per node.
   - These inputs are used in a ridge regression problem to produce a feature attribution vector for the subgraph.
   - With T subgraphs, we generate T explanations.
2. **Link Prediction:** Again, the dataset is a single graph. Subgraphs are formed by randomly selecting $n = s \cdot |\mathcal{E}^{tr}|$ edges. For each subgraph:
   - Each row in the $n \times F$ feature matrix represents the features of a single link. These features are derived by combining the feature vectors of the two nodes defining the link, using methods such as concatenation or averaging. The resulting feature vector for each link has a length of F.
   - The $n \times 1$ prediction vector contains one label per edge.
   - These inputs are used in a ridge regression problem to produce a feature attribution vector for the subgraph.
   - As with node classification, we generate T explanations for T subgraphs.
3. **Graph Classification:** For graph-level predictions, the dataset $\mathcal{D}^{tr}$ is a collection of graphs. We extend the above pattern to T collections of $n = s \cdot |\mathcal{D}^{tr}|$ subgraphs, where each subgraph is drawn from a different graph in the training set. Specifically:
   - Each subgraph in a collection is summarized by a feature vector of length F (e.g., by averaging its node or edge features).
   - For a collection of n subgraphs, we construct:
     - An $n \times F$ subgraph feature matrix, where each row corresponds to a subgraph in the collection.
     - An $n \times 1$ prediction vector, containing one prediction per subgraph.
   - These inputs are used in a ridge regression problem to produce a feature attribution vector for the collection.

- With T collections of n subgraphs, we produce T explanations.

By consistently framing each task as T groups of $n \times F$ data points, our method provides a unified approach while adapting F to the specific task requirements.

For instance, Table 8 provides sample results on graph classification using the MUTAG dataset; the results demonstrate that our method is effective beyond node classification.

Table 8: Watermarking results: graph classification

# Subgraph Collections	**4**	**5**	**6**
p-value	0.039	0.037	<0.001
Acc (train/test)	0.915/0.900	0.954/0.929	0.915/0.893

H THE USE OF LARGE LANGUAGE MODELS

In this work, large language models (LLMs) were not used in any part of the methodology, data analysis, or experiments. Their role was solely limited to polishing the language and improving the readability of the manuscript. All scientific ideas, experimental designs, and results are entirely the work of the authors.